

# Efficient Computational method using random matrices describing critical thermodynamics

Roberto da Silva<sup>1</sup>, Eliseu Venites<sup>1</sup>, Sandra D. Prado<sup>1</sup>, J. R. Drugowich de Felicio<sup>2</sup>

*1 - Instituto de Física, Universidade Federal do Rio Grande do Sul,*

*Av. Bento Gonçalves, 9500 - CEP 91501-970, Porto Alegre, Rio Grande do Sul, Brazil*

*2 - Departamento de Física, Faculdade de Filosofia Ciências e Letras de Ribeirão Preto, Universidade de São Paulo, Av. dos Bandeirantes 3900, Ribeirão Preto, São Paulo, Brazil*

Our research highlights the effectiveness of utilizing matrices akin to Wishart matrices, derived from magnetization time series data under specific dynamics, to elucidate phase transitions and critical phenomena in the Q-state Potts model. By employing appropriate statistical methods, we not only discern second-order transitions but also differentiate weaker first-order transitions through careful analysis of the density of eigenvalues and their fluctuations. Furthermore, we investigate the method's sensitivity to stronger first-order transition points. Importantly, we establish a robust correlation between the system's actual thermodynamics and the spectral thermodynamics encapsulated within the eigenvalues. Our findings are further substantiated by correlation histograms of the time series data, revealing insightful patterns. Expanding upon our core findings, we present a didactic analysis that draws parallels between the spectral properties of criticality in a spin system and matrices intentionally imbued with correlations (a toy model). Within this framework, we observe a universal behavior characterized by the distribution of eigenvalues into two distinct groups, separated by a gap dependent on the level of correlation, influenced by temperature-induced changes in the spin system.

Keywords: Random Matrices, Wishart matrix, phase transitions, critical phenomena

## I. INTRODUCTION

Fluctuation phenomena form the bedrock of understanding thermodynamics, encompassing both its processes and postulates [1–3]. While Wigner's groundbreaking research, particularly his exploration of the intricate spectra of heavy nuclei mirrored in the eigenvalues of random matrices, did not primarily delve into thermodynamics [4–7], Dyson later unveiled a profound connection. Dyson elucidated the significant link between the joint eigenvalues distribution of random matrices and the Boltzmann weight of a static Coulomb gas, characterized by a logarithmic repulsion term between the charges and a harmonic attraction term [7–10].

Despite this progress, the direct correlation between the fluctuation phenomena of specific ran-

dom matrices derived from natural systems and the thermodynamics of those systems remained elusive. Among numerous statistical concepts, correlation emerges as pivotal for understanding phase transitions and critical phenomena within Thermostatistics. Notably, Wishart [11], several decades ahead of Wigner and Dyson, delved into correlated time series. He introduced the Wishart ensemble, which encompasses random correlation matrices, diverging from the Gaussian or Unitary ensembles.

The research presents an innovative approach utilizing Wishart matrices derived from magnetization time series to analyze the thermodynamic properties of eigenvalues linked to the Potts model. The findings indicate that this method adeptly captures both first-order phase transitions and critical phenomena, primarily by examining the dispersion of eigenvalues. Moreover, supplementary analyses demonstrate, through both analytical and computational means, the distribution of eigenvalue spectra within artificially correlated Wishart matrices, revealing discernible groups with a gap influenced by correlation strength, a phenomenon presented in a manner similar to the spectra of the Potts model. Significantly, these results highlight the versatility of the proposed methodology, extending its applicability beyond critical points to encompass first-order transition points as well. However, for the stronger first-order points, the method is not obligated to work, but even so, it seems to respond satisfactorily.

For that, it is essential to establish a brief review of the literature that led to building our idea and its solution. Here we define the main object for our analysis – the matrix element  $a_{ij}$  that denotes the amount of the  $j$ -th time series at the  $i$ -th time step of a system with  $N$  different time series. Here  $i = 1, \dots, M$ , and  $j = 1, \dots, N$ . So the matrix  $A$  is  $M \times N$ . In order to analyze spectral properties, an interesting alternative is to consider not  $A$  but the square matrix  $N \times N$ :

$$G = \frac{1}{M} A^T A ,$$

such that  $G_{ij} = \frac{1}{M} \sum_{k=1}^M a_{ki} a_{kj}$ , which is the covariance matrix. It's crucial to note that  $M \geq N$ . In this context, Wishart matrices are random matrix models that describe universal aspects of covariance matrices.

At this juncture, rather than working directly with  $A$ , it becomes more advantageous to work with the matrix  $\Lambda$ , defined in terms of standard variables:

$$\Lambda_{ij} = \frac{a_{ij} - \langle a_j \rangle}{\sigma_{a_j}}, \quad (1)$$

with  $\sigma_{a_j} \approx \sqrt{\langle a_j^2 \rangle - \langle a_j \rangle^2}$ , where:  $\langle a_j^k \rangle = \frac{1}{M} \sum_{i=1}^M a_{ij}^k$  represents the  $k$ -th moment of  $j$ -column.

Thereby if  $\mathcal{G} = \frac{1}{M} \Lambda^T \Lambda$ , we have:

$$\begin{aligned} \mathcal{G}_{ij} &= \frac{1}{M} \sum_{k=1}^M \frac{a_{ki} - \langle a_i \rangle}{\sqrt{\langle a_i^2 \rangle - \langle a_i \rangle^2}} \frac{a_{kj} - \langle a_j \rangle}{\sqrt{\langle a_j^2 \rangle - \langle a_j \rangle^2}} \\ &= \frac{\langle a_i a_j \rangle - \langle a_i \rangle \langle a_j \rangle}{\sigma_{a_i} \sigma_{a_j}}, \end{aligned} \quad (2)$$

where  $\langle a_i a_j \rangle = \frac{1}{M} \sum_{k=1}^M a_{ki} a_{kj}$ , i.e.,  $\mathcal{G}$  is the correlation matrix. Analytically, if  $\Lambda_{ij}$  ( $a_{ij}$ ) are independent random variables, thus we have the so called Wishart orthogonal ensemble (WOE). On the other hand, many authors consider to understand the role of correlations and in that case, it is interesting to consider the one-sided correlated Wishart orthogonal ensemble (CWOE) [12, 13] and in this case  $\Lambda^T = \Omega^{1/2} B^T$  where  $\Omega$  is a real symmetric positive definite non-random  $N \times N$  matrix that accounts for the correlations in time series (columns) of data matrix  $\Lambda$  and  $B$  is composed by independent random variables with average 0 and variance 1. In this case

$$\mathcal{G} = \frac{1}{M} \Lambda^T \Lambda = \frac{1}{M} \Omega^{1/2} B^T B \Omega^{1/2}$$

which implies:

$$\text{Tr}\left(\frac{1}{M} B^T B\right) = \text{Tr}\left(\frac{1}{M} \Omega^{-1} \Lambda^T \Lambda\right) = \text{Tr}(\Omega^{-1} \mathcal{G}) \quad (3)$$

Now we know that the joint probability density of the matrix elements of  $B^T$  can be written considering gaussian distribution (no loss of generality) for these entries:

$$\begin{aligned} P(B_{11}, B_{12}, \dots, B_{MN}) dB &= \prod_{i=1}^N \prod_{j=1}^M P(B_{ji}) dB_{ji} \\ &= \frac{\exp\left(-\frac{1}{2} \sum_{i=1}^N \sum_{j=1}^M B_{ji}^2\right)}{(2\pi)^{NM/2}} dB \\ &= \frac{\exp\left(-\frac{1}{2} \sum_{i=1}^N [B^T B]_{ii}\right)}{(2\pi)^{NM/2}} dB \\ &= \frac{\exp\left[-\frac{1}{2} \text{Tr}(B^T B)\right]}{(2\pi)^{NM/2}} dB \end{aligned} \quad (4)$$

where  $dB = \prod_{i=1}^N \prod_{j=1}^M dB_{ji}$ .

Based on the equations 3 and 4 to write the joint probability density for elements of  $\mathcal{G}$  supposes to calculate a Jacobian from  $M \times N$  variables:  $\{B_{11}, B_{12}, \dots, B_{MN}\}$  to  $N \times N$  variables:  $\{\mathcal{G}_{11}, \mathcal{G}_{12}, \dots, \mathcal{G}_{NN}\}$  which was performed by Wishart [11] and revisited by other authors (for exam-

ple: [14, 15]) which is given by:

$$P(\mathcal{G}_{11}, \dots, \mathcal{G}_{NN})d\mathcal{G} = K_N \det(\Omega)^{-\frac{M}{2}} \det(\mathcal{G})^{\frac{(M-N-1)}{2}} \times \exp\left[-\frac{M}{2} \text{tr}(\Omega^{-1}\mathcal{G})\right] d\mathcal{G} \quad (5)$$

where  $d\mathcal{G} = \prod_{i=1}^N \prod_{j>i}^N d\mathcal{G}_{ij} \times \prod_{i=1}^N d\mathcal{G}_{ii}$ .

From that distribution we can obtain the jointly distribution of eigenvalues of  $\mathcal{G}$ . In the particular case of  $\Omega = 1$ , i.e.,  $\Lambda = B$ , the jointly distribution of eigenvalues is described by the Boltzmann weight [12, 16]:

$$P(\lambda_1, \dots, \lambda_N) = C_N \exp\left[-\frac{M}{2} \sum_{i=1}^N \lambda_i + \frac{M-N-1}{2} \sum_{i=1}^N \ln \lambda_i + \sum_{i<j} \ln |\lambda_i - \lambda_j|\right] \quad (6)$$

where  $C_N^{-1} = \int_0^\infty \dots \int_0^\infty d\lambda_1 \dots d\lambda_N \exp[-H(\lambda_1 \dots \lambda_N)]$ , corresponding to the Hamiltonian:

$$\mathcal{H}(\lambda_1 \dots \lambda_N) = \frac{M}{2} \sum_{i=1}^N \lambda_i - \frac{(M-N-1)}{2} \sum_{i=1}^N \ln \lambda_i - \sum_{i<j} \ln |\lambda_i - \lambda_j| \quad (7)$$

at temperature  $\beta^{-1} = 1$ . The last term is a logarithmic repulsion exactly as the standard Wigner/Dyson ensembles.

Marchenko and Pastur [17] showed that the density of eigenvalues here written as:

$$\sigma(\lambda) = \int_0^\infty \dots \int_0^\infty P(\lambda, \lambda_2, \dots, \lambda_N) d\lambda_2 \dots d\lambda_N \quad (8)$$

of the matrix  $\Phi = \frac{1}{M} \Lambda^T \Lambda$ , for the particular case  $\Omega = 1$ , follows the known Marcenko-Pastur distribution and not the standard semi-circle law, described as:

$$\sigma(\lambda) = \begin{cases} \frac{M}{2\pi N} \frac{\sqrt{(\lambda - \lambda_-)(\lambda_+ - \lambda)}}{\lambda} & \text{if } \lambda_- \leq \lambda \leq \lambda_+ \\ 0 & \text{otherwise} \end{cases} \quad (9)$$

where

$$\lambda_{\pm} = 1 + \frac{N}{M} \pm 2\sqrt{\frac{N}{M}}. \quad (10)$$

It is imperative to underscore that, within the framework of the Gaussian random matrix model, a fundamental assumption is the existence of the first four moments. This assumption implies

that the presence of Levy tails in the time series should not exhibit excessive heaviness. The presence of the third and fourth moments holds particular significance as it enables control over the statistical characteristics of the largest eigenvalues, ensuring their alignment with the Gaussian random matrix model. This phenomenon is extensively documented in the context of convergence to the Marchenko-Pastur law, as exemplified in the work of Gotze and Tikhomirov [21]. It is worth noting that the requirement for the fourth moment is not a mere technical constraint; it plays a pivotal role in achieving convergence, especially at the spectral edges.

However, the problem is highly complicated in the general case ( $\Omega \neq 1$ ), and the spectra do not precisely follow a simple closed form. Closed forms were interestingly obtained by Guhr and collaborators using supersymmetric methods [18]. They also used similar approach to study the statistics of the smallest eigenvalues [19]. An even more detailed result is presented in Sections III and IV of the work by Wirtz et al. [20]. Prior to that, the connection between random matrices and critical phenomena had other important actors.

Some interesting contributions in the late 1980s and early 1990s (see, for example, [22, 23]) explored the relationship between critical properties of statistical mechanics models in equilibrium and the spectral density of random matrices. It is also known that the largest eigenvalue of a complex Gaussian sample covariance matrix, as well as others, such as those from the Gaussian family, exhibit sharp phase transitions, which have been studied in the literature (see, for example, [24, 25]).

In an exciting application of random matrices the authors in [26–28], and simultaneously and independently in [29, 30] using the results developed by Marcenko and Pastur [17, 31], showed that deviations from the bulk of spectra of random correlation matrices built with financial market assets are related to genuine correlations from Stock Market. Emphasizing the significance of exploring the structure of covariance matrices in Principal Component Analysis is paramount, as demonstrated by seminal works such as [32].

Interestingly, some authors investigated spectral properties of correlation matrices in near-equilibrium phase transitions [33]. In this case, they studied correlation matrices of the  $N = L^2$  spins of the Ising model in the two-dimensional lattice under  $\tau$  time steps of evolution to evidence of the power-law spatial correlations at a phase transition display. Similarly, the authors in [34] explored results in the steady-state for the correlation matrix of the asymmetric simple exclusion process.

However, besides the body of results in this field, we are far from grasping all the information about phase transitions in spin systems. They seem to be inherent to the system even in its initial

stages of evolution [35, 36]. When suddenly placed at finite temperatures, a system initially at high temperatures responds to the natural pre-existent natural correlations in the interacting system. For instance, it can explain the richness of the time evolution of magnetization [37, 38].

In this context, the most relevant theories consider that the critical behavior of the statistical mechanics systems can be captured before the system reaches the equilibrium, and scaling relations that consider initial conditions were used to obtain critical exponents and parameters (see, for example: [35–41]). These results motivated several other approaches in different systems with and without defined Hamiltonian, and mean-field systems (only to mention some relevant contributions: [42–47]).

Recently, one of the authors of this current work showed that random matrices could enlighten critical phenomena by showing that the density of eigenvalues strongly responds to the criticality of the system in a simple model as the two-dimensional Ising model [48]. Motivated by this result, the question which arises is if the phase transitions are imprinted into the properties of random matrices simulated via Monte Carlo (MC) from time evolutions far from thermalization. Moreover, another question to be answered is whether such a method works only for critical points or can also be extended for first-order transition points. If extendable, are there fundamental or universal aspects that go beyond spin models and are also characterized by the correlations existing in time series, not only in the magnetization time series?

In this paper, we give a positive answer to this question and supply the fundamentals to understand how the eigenvalues density of random matrices governs the phase transition points of the Potts model. We show that the method describes very well the critical (second-order) points of the Potts model which was its initial proposal for the Ising model in both short and long-range mean field Ising model [48, 49], but surprisingly the method works very well for the a weak first order point  $Q = 5$ . For  $Q \geq 7$  (stronger first order points) the method seems to respond for amounts based on upper fluctuations of eigenvalues but it presents deviations for the expect value  $\langle \lambda \rangle$ . It is important to note, to the best of our knowledge, that methods for second and first order are applied distinctly in the literature, and the method here presented has no obligation to work for strong first order which will deserves attention in other alternative study.

In addition, we show how the artificially correlated system's spectra explain the existence of two groups of eigenvalues separated by a gap that depends on the strength of the correlation. This gap dependence on the correlation is the key to understanding what occurs for the critical and first-order phenomena.

We thus provide an affirmative response to this pivotal question and lay the foundational ground-

work for comprehending how the eigenvalue density of random matrices governs the phase transition points of the Potts model. Our method excels in accurately characterizing the critical (second-order) points of the Potts model, originally proposed for the Ising model, both in the short and long-range mean field Ising model, as documented in [48, 49]. Remarkably, our method also proves effective in capturing a weak first-order point at  $Q = 5$ .

For cases where  $Q \geq 7$ , corresponding to stronger first-order phase transitions, our method exhibits sensitivity to the dispersion of eigenvalues and yields insights from this metric. However, it exhibits deviations in the expectation value  $\langle \lambda \rangle$ . It is worth emphasizing that, to the best of our knowledge, methods for second-order and first-order phase transitions are typically distinct in the literature. Our method, as presented here, is not inherently designed to handle strong first-order transitions, which warrant further exploration in alternative studies.

Additionally, we elucidate how the spectra of artificially correlated systems shed light on the existence of two distinct groups of eigenvalues, separated by a gap whose magnitude is contingent upon the strength of the correlation. This gap's dependence on the correlation strength holds the key to comprehending the behaviors associated with critical and first-order phenomena.

We first performed preparatory results about the spectral properties of random matrices built from correlated time series pair-by-pair, considering a simple way to fix the correlation. We then explored the emergence of the gap of eigenvalues and how this influences the fluctuation spectra from simple analytical cases and after with MC simulations. Such a study is presented in the next section (Sec. II).

In section III, we present the details about how to build the Wishart matrices of the time series of magnetization for the Potts model. Since we observed how the correlations between time series could influence the density of eigenvalues in Sec. II, we then performed simulations for the Potts model from  $q = 3$  up to  $q = 10$  by showing how the spectra of random matrices built from magnetization time series can precisely indicate the transition points and, most importantly, independently from the transition order since we migrate from critical points passing by weak first-order points until strong first-order transition. We present our main results in section IV.

To support our results even more, we analyzed the histograms of correlations between the different evolutions, i.e., the histogram of elements of Wishart matrices, and observed how such histograms are linked to the density of eigenvalues.

The gap in the distribution of eigenvalues seems to govern the existence of phase transitions but not in a straightforward way, and this can be observed in even simpler situations, i.e., not for a physical system, but for a system artificially built, as suggested by the spectra studied in the

preparatory section (Sec. II)

The main contribution of this work is strongly based on the proposal of a spectral thermodynamics built from Wishart matrices that can reflect the real thermodynamics of spin systems.

## II. CORRELATIONS AND WISHART MATRICES: A PREPARATORY STUDY

In this section, we show the role played by correlations in the emergence of a gap in the distribution of the eigenvalues of Wishart matrices is the eigenvalues of Wishart matrices. For that, we build Wishart matrices by artificially correlating columns of the matrix  $A$  by pairs. A simple way to correlate two random variables is the one used by us in two previous papers. One to correlate phases of waves to observe the emerging of rogue waves [50] and a second to spatially correlate points in the traveling salesman problem to analyze the loss of performance of simulated annealing from two to one dimension [51]. Consider two independent and identically distributed (i.i.d.) random variables  $\varphi_1$  and  $\varphi_2$  with  $\langle \varphi_1 \rangle = \langle \varphi_2 \rangle = 0$ . Then, two  $\rho$ -correlated variables can be obtained by making  $\phi_1 = \varphi_1 \sin \theta + \varphi_2 \cos \theta$  and  $\phi_2 = \varphi_1 \cos \theta + \varphi_2 \sin \theta$ , if:

$$\rho = \frac{\langle (\phi_1 - \langle \phi_1 \rangle) (\phi_2 - \langle \phi_2 \rangle) \rangle}{\sqrt{\langle (\Delta \phi_1)^2 \rangle \langle (\Delta \phi_2)^2 \rangle}} = \sin 2\theta. \quad (11)$$

where we assume the existence of the second moments of  $\phi_1$  and  $\phi_2$ , i.e.,  $0 < \langle (\Delta \phi_1)^2 \rangle < \infty$  and  $0 < \langle (\Delta \phi_2)^2 \rangle < \infty$ , with  $\langle (\Delta \phi_1)^2 \rangle = \langle \phi_1^2 \rangle - \langle \phi_1 \rangle^2$ , and  $\langle (\Delta \phi_2)^2 \rangle = \langle \phi_2^2 \rangle - \langle \phi_2 \rangle^2$ .

In order to understand the role played by  $\rho$  on the spectra of  $\mathcal{G}$ , we build matrices  $A$  where each pair of adjacent columns are composed by two vectors  $\mathbf{a}_i = [a_{i,1} \dots a_{i,M}]^t$  and  $\mathbf{a}_{i+1} = [a_{i+1,1} \dots a_{i+1,M}]^t$ , such that:  $a_{k,i} = \varphi_{k,i}^{(1)} \sin \theta + \varphi_{k,i}^{(2)} \cos \theta$ , while  $a_{k,i+1} = \varphi_{k,i}^{(1)} \cos \theta + \varphi_{k,i}^{(2)} \sin \theta$  (recall that this is not a rotation). It follows straightforward from the fact that  $\varphi_{i,k}^{(1)}$  and  $\varphi_{i,k}^{(2)}$  are  $\rho$ -correlated random variables that  $a_{k,i}$  and  $a_{k,i+1}$  are also two  $\rho$ -correlated random variables with average zero and variance one.

By choosing  $\varphi_{i,k}^{(1)}$ ,  $\varphi_{i,k}^{(2)}$ ,  $k = 1, \dots, M$ , random variables  $N[0,1]$  we build matrices where some columns are correlated. For  $N = 2$ , we certainly guarantee that the correlation between the columns is  $\rho$ . Particularly for  $M = 2$ , the elements are:

$$\mathcal{G}_{11} = \varphi_{1,1}^{(1)2} \sin^2 \theta + \varphi_{1,1}^{(2)2} \cos^2 \theta + 2\varphi_{1,1}^{(1)}\varphi_{1,1}^{(2)} \sin \theta \cos \theta \quad (12)$$

such that  $\langle \mathcal{G}_{11} \rangle = 1$ , since  $\langle \varphi_{1,1}^{(1)2} \rangle = \langle \varphi_{1,1}^{(2)2} \rangle = 1$  and  $\langle \varphi_{1,1}^{(1)}\varphi_{1,1}^{(2)} \rangle = \langle \varphi_{1,1}^{(1)} \rangle \langle \varphi_{1,1}^{(2)} \rangle = 0$ . In that same way, we can conclude that:  $\langle \mathcal{G}_{12} \rangle = \langle \mathcal{G}_{21} \rangle = 2 \sin \theta \cos \theta = \rho$  and  $\langle \mathcal{G}_{22} \rangle = 1$ . It follows that the eigenvalues of  $\langle \mathcal{G} \rangle$  in this case are  $\lambda_{\pm} = 1 \pm \rho$ .



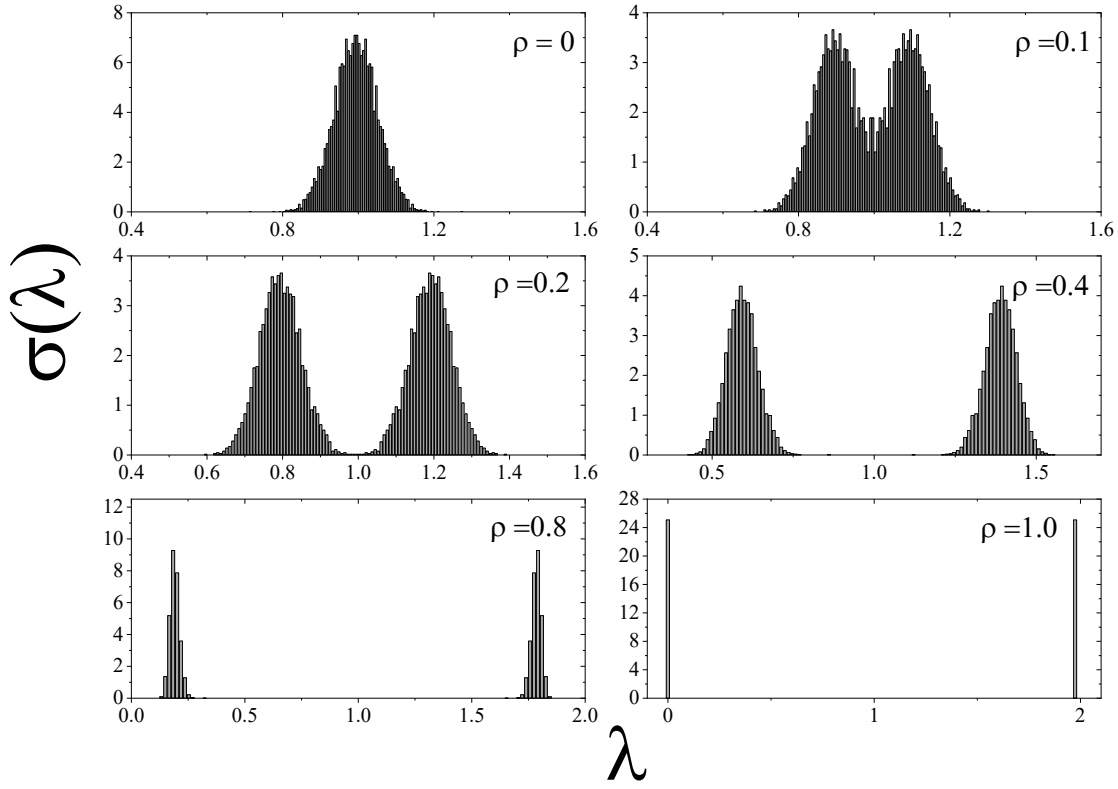


Figure 1. Density of eigenvalues  $\mathcal{G}$  for different values of  $\rho$  considering an ensemble of  $N_{run} = 4000$  different matrices. The pairwise columns of  $A$  ( $\mathcal{G} = \frac{1}{M} \Lambda^t \Lambda$ ) are  $\rho$ -correlated according to our procedure. We used  $N = 2$  and  $M = 300$ .

For an arbitrary  $M$ , one has a block-diagonal matrix written as

$$\langle \mathcal{G} \rangle = \begin{pmatrix} 1 & \rho \\ \rho & 1 \end{pmatrix} \otimes \mathbf{I}_{N/2 \times N/2} \quad (13)$$

and the eigenvalues of  $\langle \mathcal{G} \rangle$  are similarly  $\lambda_{\pm} = 1 \pm \rho$  with multiplicity  $N/2$ . However, the situation is quite different in the case of an ensemble of matrices  $G$  corresponding to the different values of  $\varphi_{i,k}^{(1)}$  and  $\varphi_{i,k}^{(2)}$  for  $k = 1, \dots, M$  and  $i = 1, \dots, N/2$ . By instance, for  $M = 300$  and  $N = 2$ , with  $N_{run} = 4000$  different matrices  $\mathcal{G}$ , the density of eigenvalues  $\sigma(\lambda)$  is two-peaked. The peaks are in  $1 - \rho$  and other in  $1 + \rho$  as illustrated in Fig. 1, in agreement with the result obtained for  $\langle \mathcal{G} \rangle$  for the case of  $M = 2$ .

However, this is not true for  $N = 100$ . In this case, for  $\rho = 0$  and  $N$  large, the density of eigenvalues must behave as a Marchenko-Pastur law and not only two eigenvalues with multiplicity

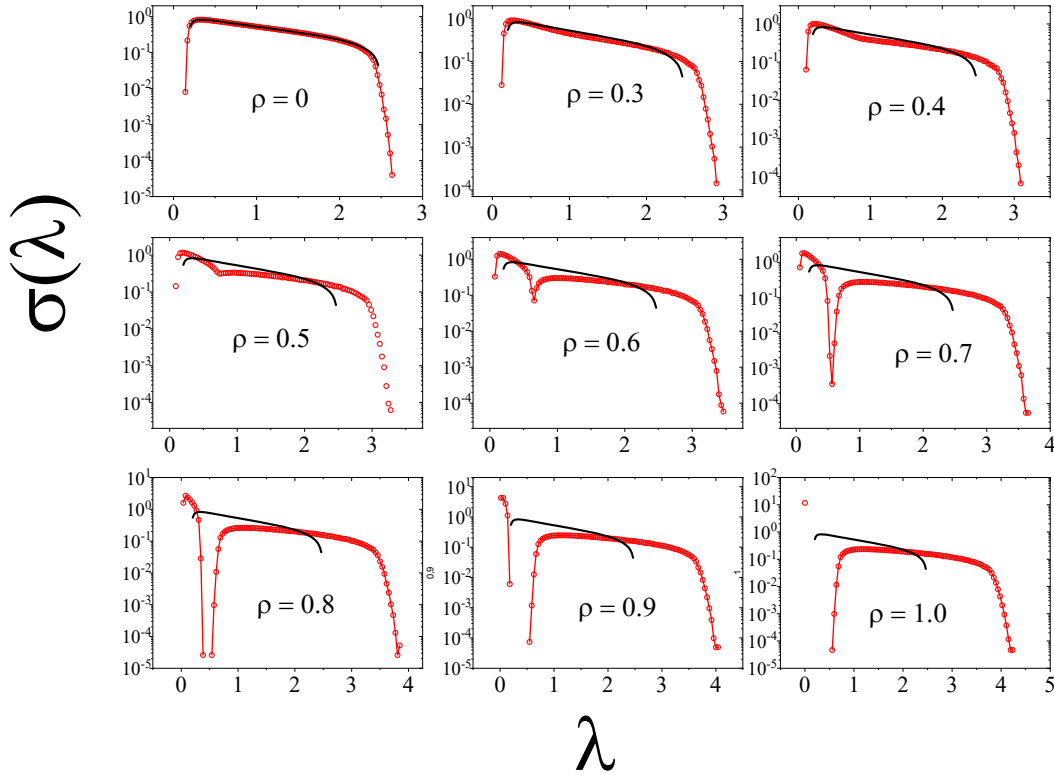


Figure 2. Density of eigenvalues considering an ensemble of  $N_{run} = 4000$  different matrices  $\mathcal{G}$  for different values of  $\rho$ . The pairwise columns of  $A$  ( $\mathcal{G} = \frac{1}{M}\Lambda^t\Lambda$ ) are  $\rho$ -correlated according to our procedure. We used  $N = 100$  and  $M = 300$ . The continuous curve corresponds to the Marchenko-Pastur density of eigenvalues.

$N/2$ . Then, it is important to check what happens for  $\rho > 0$  and  $N$  large.

Fig. 2 shows that as  $\rho$  increases, the density of eigenvalues becomes distinguished from the Marchenko-Pastur prediction, as expected. We also observe a singularity that becomes more pronounced as  $\rho$  increases. This discontinuity gives origin to a gap between  $\rho = 0.7$  and  $\rho = 0.8$ . This gap enlarges as  $\rho$  increases until one of the branches disappears ( $0.9 < \rho < 1.0$ ). Here, the effective correlation is not exactly  $\rho$  since when crossing columns of no adjacent columns, the correlation is zero on average (or 1 between the same columns). On the other hand, it is a fact that when  $\rho$  increases, the effective correlation also increases.

To examine the influence of correlation  $\rho$  on eigenvalue fluctuations, we plotted  $\langle\lambda\rangle$  and  $\zeta = \frac{d}{d\rho}\langle(\Delta\lambda)^2\rangle$  as functions of  $\rho$ , where  $\langle(\Delta\lambda)^2\rangle = \langle\lambda^2\rangle - \langle\lambda\rangle^2$  is the dispersion of the eigenvalues. Notably, we observed that at  $\rho \approx 0.9$ , there was a maximum value of  $\langle\lambda\rangle$  and a corresponding

minimum value of  $\zeta$  (refer to Fig. 3). In Fig. 2, we can observe an interesting competition in the evolution of eigenvalue density: as  $\rho$  increases, the singularity previously mentioned causes the density of eigenvalues near the origin ( $\lambda \approx 0$ ) to increase while the bulk of eigenvalues on the right side of the singularity slightly shifts to the right. The former phenomenon appears to have a stronger effect than the latter as  $\rho$  increases, leading to a decrease in the average eigenvalue until  $\rho \approx 0.9$ . However, an inversion is observed for  $\rho > 0.9$ , where the average eigenvalue increases due to a stagnation of null eigenvalues caused by the high correlation and the right shift being more preponderant. The derivative of the dispersion of eigenvalues seems to follow this trend, decreasing for  $\rho > 0.9$  after an initial increase leading up to this value.

It's worth noting that Figure 2 indicates a superposition of two Marchenko-Pastur laws, which becomes evident once two distinct spectral bulks have been identified, as observed by Wirtz, Kieburg, and Guhr [20].

This behavior implies that eigenvalues are correlated, and their dependence on these correlations can be quantified by examining their fluctuations. It is worth noting that this pedagogical study bears resemblances to significant prior findings in the literature, specifically the spiked (Wishart) random matrix ensemble, as discussed in references [52–55]. Furthermore, it is advisable to verify the results presented here by comparing them to the analytical outcomes in [20].

Using such motivation, we will consider now, Wishart matrices built from time series of magnetization of the Potts model for an arbitrary number of states  $Q$ .

We will show that we can identify phase transitions using the fluctuations of eigenvalues of such matrices and that in this particular case, the minimum of average eigenvalue occurs at the proximity of the transition point, as well as an inflection point in the variance of eigenvalue.

Still, we also illustrate that our results are supported by monitoring the histograms of correlation at different temperatures of the system.

### III. POTTS MODEL AND WISHART MATRICES

The Hamiltonian of the  $d$ -dimensional  $Q$ -state Potts model (see for example [56]) can be written as

$$\beta\mathcal{H}_{\text{Potts}} = -K \sum_{\langle i,j \rangle} \delta_{s_i, s_j} \quad (14)$$

where  $\beta = (k_B T)^{-1}$ , with  $k_B$  being the Boltzmann constant,  $T$  is the system's temperature, and  $K$  is the coupling coefficient. Here  $\langle i, j \rangle$  indicates that the sum is taken over all nearest neighbor sites,

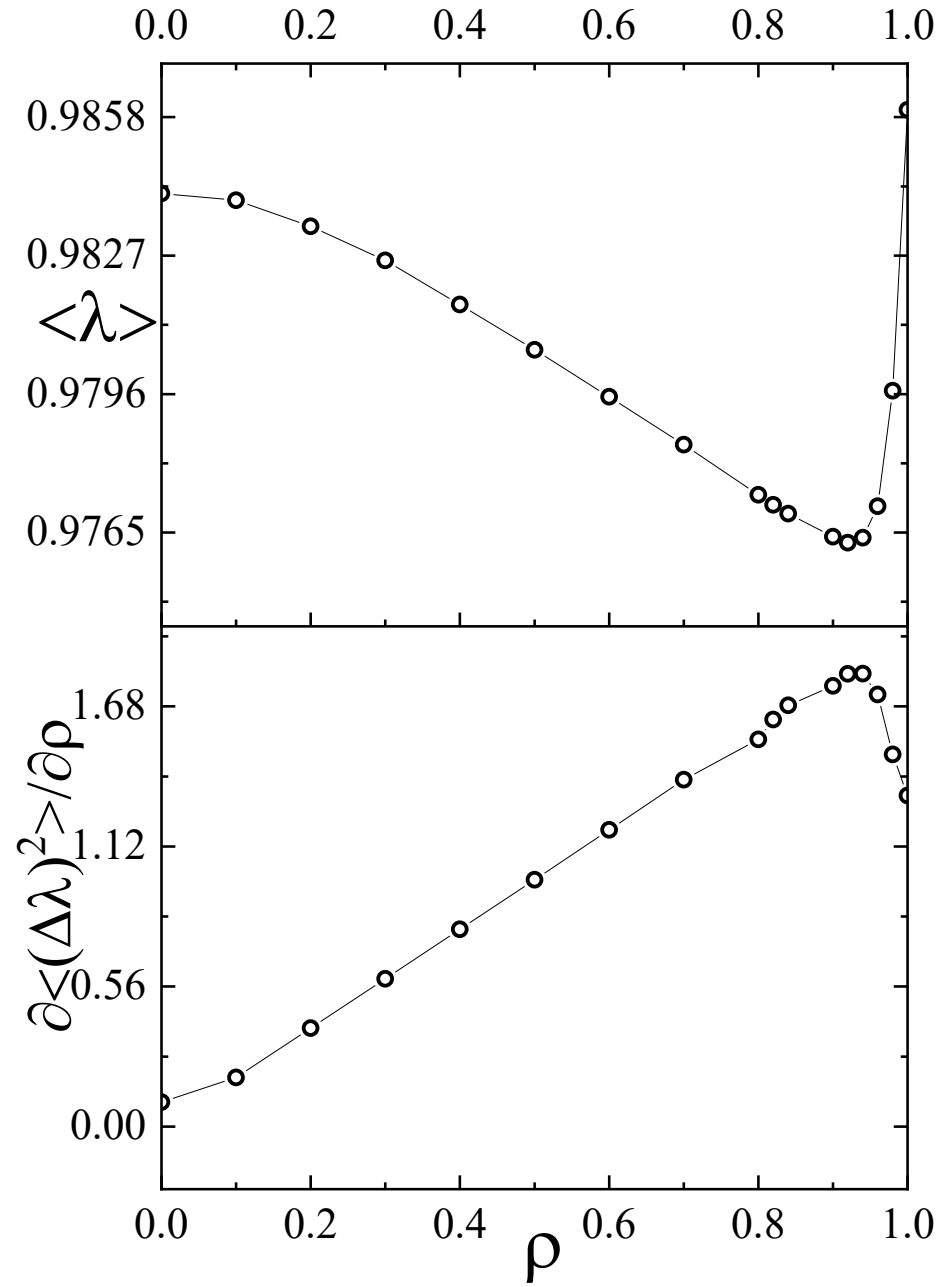


Figure 3. Eigenvalue average and derivative of eigenvalue dispersion as a function of the  $\rho$ . Extremals are observed for  $\rho_c \approx 0.9$ .

and  $s_i = 0, 1, \dots, Q - 1$ . The system presents a phase transition for  $T_C = K_C^{-1} = (\ln(1 + \sqrt{Q}))^{-1}$  which is continuous (second order) for  $Q \leq 4$  and discontinuous (first order) for  $Q \geq 5$ .

In addition to the many equilibrium studies of the Potts model, some authors explored its critical dynamics [57, 58]. A non-equilibrium version of the model, driven out of equilibrium by coupling the spins to heat baths at two different temperatures presents entropy production, as the authors interestingly showed in [59].

Thus, now, we define the main object for our current analysis, the magnetization matrix element:

$$\mathcal{M}_{tj} = \frac{1}{L^d(q-1)} \sum_{k=1}^{L^d} (q\delta_{s_k(t,j),1} - 1) \quad (15)$$

where  $s_k(t, j)$  denotes the state of  $k$ -th spin of the  $j$ th time series at the  $t$ th MC step of a system with  $L^d$  spins (in this work, for simplicity, we used  $d = 2$ , the minimal dimension to appear phase transition in the Potts model). Here  $t = 1, \dots, N_{MC}$ , and  $j = 1, \dots, N_{run}$ . In this same equation,  $\delta_{\mu,\nu}$  denotes the Kronecker delta symbol, which assumes a value equal to 1 if  $\mu = \nu$  and 0 otherwise. So the magnetization matrix  $\mathcal{M}$  is  $N_{MC} \times N_{run}$ . Similarly, we define:  $\mathcal{M}_{tj}^* = \frac{\mathcal{M}_{tj} - \langle \mathcal{M}_j \rangle}{\sqrt{\langle \mathcal{M}_j^2 \rangle - \langle \mathcal{M}_j \rangle^2}}$ , exactly as we previously described and thus we obtain the Wishart matrix  $\mathcal{G} = \frac{1}{N_{MC}} \mathcal{M}^{*T} \mathcal{M}^*$ .

Here it is important to elucidate a pivotal calculation that shows what we are exactly with these matrices with more details. Consider two distinct time evolutions, denoted as  $\mathcal{M}_{tk}$  and  $\mathcal{M}_{tl}$ ,  $t = 1, \dots, N_{MC}$  are two different time evolutions of the magnetization per spin. In this scenario, we can write in a more general way:

$$\mathcal{M}_{tk} = \frac{1}{L^2} \sum_{i=1}^{L^2} \sigma_{t,k,i}, \quad (16)$$

where  $\sigma_{t,k,i}$  represents the value associated with the  $i$ -th spin variable in the  $k$ -th evolution or run at time  $t$ . For example for the Potts model,  $\sigma_{t,k,i} = \frac{1}{(q-1)}(q\delta_{s_i(t,k),1} - 1)$

We can establish the correlation between these two time series through the following definition:

$$\begin{aligned}
\langle \mathcal{M}_k \mathcal{M}_l \rangle_t &= \frac{1}{N_{MC}} \sum_{t=1}^{N_{MC}} \mathcal{M}_{tk} \mathcal{M}_{tl} \\
&= \frac{1}{L^4 N_{MC}} \sum_{t=1}^{N_{MC}} \left( \sum_{i=1}^{L^2} \sigma_{t,k,i} \right) \left( \sum_{j=1}^{L^2} \sigma_{t,l,j} \right) \\
&= \frac{1}{L^4 N_{MC}} \sum_{t=1}^{N_{MC}} \left( \sum_{i=1}^{L^2} \sigma_{t,k,i} \sigma_{t,l,i} + \sum_{i \neq j=1}^{L^2} \sigma_{t,k,i} \sigma_{t,l,j} \right) \\
&= \frac{1}{L^4} \sum_{i=1}^{L^2} \left[ \left( \frac{1}{N_{MC}} \sum_{t=1}^{N_{MC}} \sigma_{t,k,i} \sigma_{t,l,i} \right) + \sum_{i \neq j=1}^{L^2} \left( \frac{1}{N_{MC}} \sum_{t=1}^{N_{MC}} \sigma_{t,k,i} \sigma_{t,l,j} \right) \right] \\
&= \frac{1}{L^4} \sum_{i=1}^{L^2} \langle \sigma_{k,i} \sigma_{l,i} \rangle_t + \frac{1}{L^4} \sum_{i \neq j=1}^{L^2} \langle \sigma_{k,i} \sigma_{l,j} \rangle_t
\end{aligned} \tag{17}$$

Given that  $\sum_{i=1}^{L^2} \langle \sigma_{k,i} \sigma_{l,i} \rangle_t = O(L^2)$ , and  $\sum_{i \neq j=1}^{L^2} \langle \sigma_{k,i} \sigma_{l,j} \rangle_t = O(L^4)$ , if we assume a moderate strength of alignments among spins in both space and time we have:

$$\langle \mathcal{M}_k \mathcal{M}_l \rangle_t \approx \left\langle \frac{1}{L^4} \sum_{i \neq j=1}^{L^2} \sigma_{k,i} \sigma_{l,j} \right\rangle_t = \langle \sigma_k \otimes \sigma_l \rangle_t.$$

When  $T > T_C$ ,  $\langle \mathcal{M}_k \rangle_t \approx 0$ . This leads to:  $\langle \mathcal{M}_k \mathcal{M}_l \rangle_t - \langle \mathcal{M}_k \rangle_t \langle \mathcal{M}_l \rangle_t \approx \frac{1}{L^4} \langle \sigma_k \otimes \sigma_l \rangle_t$ , and we can express the correlation coefficient (our matrix element of  $\mathcal{G}$ ) as:

$$\begin{aligned}
\mathcal{G}_{kl} &\approx \frac{\langle \mathcal{M}_k \mathcal{M}_l \rangle_t}{\sqrt{\langle \mathcal{M}_k^2 \rangle_t} \sqrt{\langle \mathcal{M}_l^2 \rangle_t}} \\
&\approx \frac{\langle \mathcal{M}_k \mathcal{M}_l \rangle_t}{\langle \mathcal{M}_k^2 \rangle_t} \\
&= \frac{\langle \sigma_k \otimes \sigma_l \rangle_t}{\langle \sigma_k \otimes \sigma_k \rangle_t} \approx \frac{\langle \sigma_k \otimes \sigma_l \rangle_t}{\langle \sigma_l \otimes \sigma_l \rangle_t}
\end{aligned}$$

where  $\sigma_k \equiv (\sigma_{k,1}, \dots, \sigma_{k,N})$  and  $\sigma_l \equiv (\sigma_{l,1}, \dots, \sigma_{l,N})$ . Thus  $\mathcal{G}_{kl}$  for  $T > T_C$  is determined by:

$$\mathcal{G}_{kl} \approx \frac{\langle \sigma_k \otimes \sigma_l \rangle_t}{\langle \sigma_l \otimes \sigma_l \rangle_t}$$

This metric assesses the relationship between the temporal averages of spatial correlations in both inter and intra time series. By analyzing both spatial and temporal dimensions, it presents an intriguing avenue for investigating spin systems.

Undoubtedly, being  $\mathcal{M}_{ij}$  the average magnetization (Eq. 15), then we expect that for  $T \gg T_c$  the density of eigenvalues  $\sigma^{\text{exp}}(\lambda)$  obtained from computational simulations approaches  $\sigma(\lambda)$  in Eq. 9. The interesting question is what happens when  $T \approx T_C$ . More than that, we will use the

density  $\sigma^{\text{exp}}(\lambda)$ , the one obtained from computer simulations, to obtain the critical parameter of spin models. We will show that the results here go beyond the Ising model (already studied with a similar approach [48]) since they give an account of the first-order points in addition to the critical ones.

#### IV. MAIN RESULTS

We performed MC simulations to obtain the eigenvalues of an ensemble of  $N_{run} = 4000$  different random matrices  $\mathcal{G}$  obtained from  $N_{sample} = 1000$  time evolutions of  $q$ -state Potts model of the  $N_{MC} = 300$  first MC steps of evolution at temperature  $T$ . We start with a system at infinite temperature (spins randomly chosen) and simulated according to Metropolis algorithm for systems of linear dimension  $L = 128$  (large enough here as discussed for the Ising model in [48]).

Just like it was done in Section II, the eigenvalues of the ensemble of matrices were grouped. The maximum and minimum among all of the eigenvalues of the ensemble defined the interval that was divided into a fixed number of bins:  $N_{bins} = 100$ . Thus we plotted the shape of the density of states for different temperatures.

We start our discussion by showing the density of states for  $Q = 3$  with three different temperatures. They are illustrated in Fig. 4. The density changes its shape as temperature increases. There is a gap between two groups of eigenvalues for temperature below the critical temperature ( $T = 1/2T_C$ ). The gap vanishes above the critical temperature ( $T = 1.05T_C$ ). More precisely, the gap is smaller as  $T$  approaches  $T_C$ , and it vanishes for temperatures close to the critical temperature as reported for the case  $Q = 2$  (see [48]).

For high temperatures, we observe a better approximation for the Marchenko-Pastur (red curve) in the plot corresponding to  $T = 6.5T_C$ , since the system becomes uncorrelated. However not by the tail that differs on the Marchenko-Pastur law. This occurs because we consider the correlation between the total magnetization not extracting the autocorrelation spin-spin that generate this distinct tail in relation to expect law. It is important to mention that it is not importance to the working of the method.

Recall that time evolutions start from initial conditions at infinite temperatures, i.e. spins are randomly chosen with the same probability.

It is important to observe the Gaussian behavior centered at  $\lambda = 73$  in Figure 4, which occurs at  $T = T_C/2$ . This is better highlighted in a linear scale (see Figure 5).

The phenomenon is intriguing because there is a single eigenvalue in each sample that departs

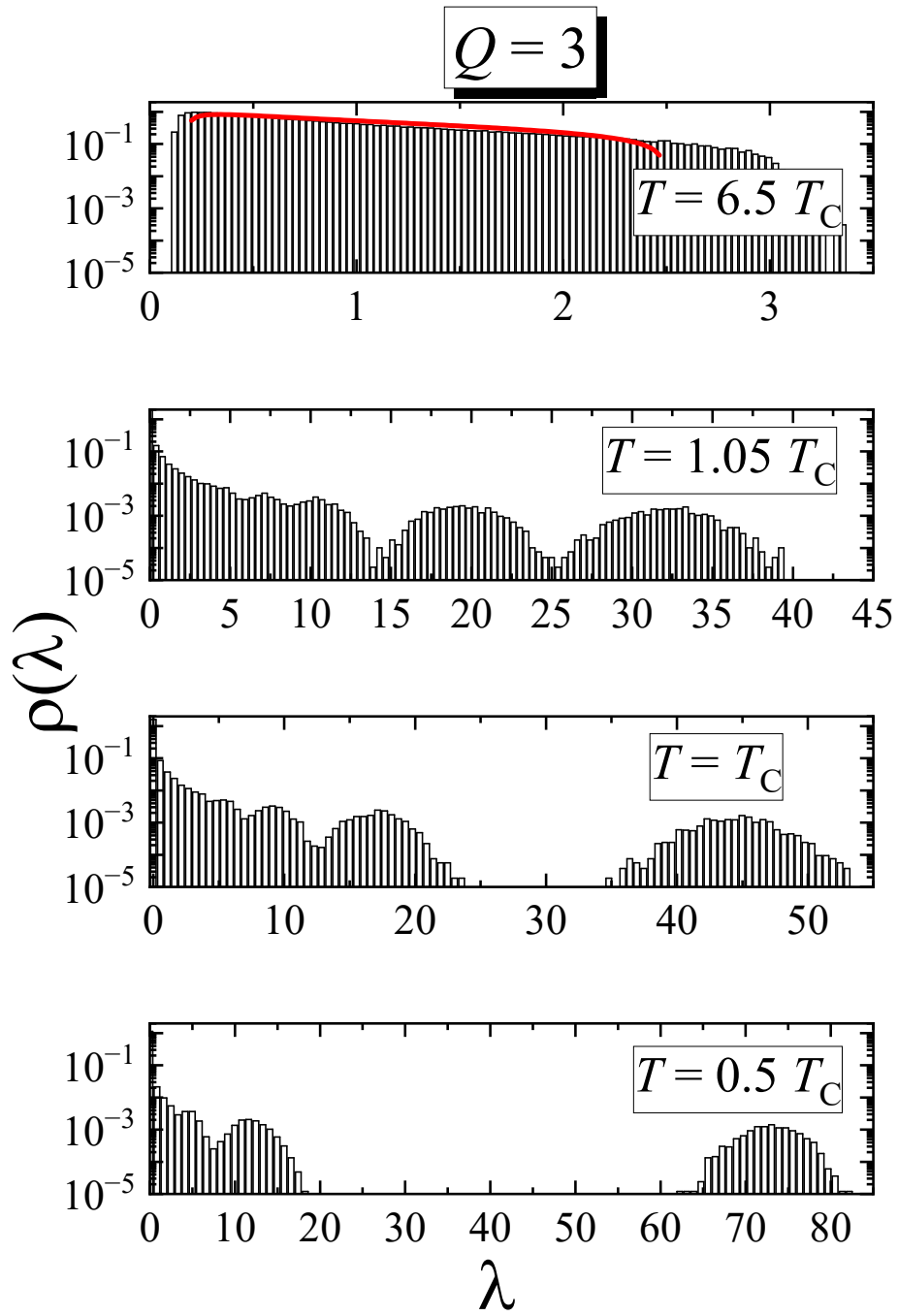


Figure 4. Density of eigenvalues for 3-state Potts model. The gap between eigenvalues disappears after  $T > T_C$  as previously observed for the Ising model (see [48]). A good approximation with Marchenko-Pastur law (red continuous curve) is observed for high temperatures.



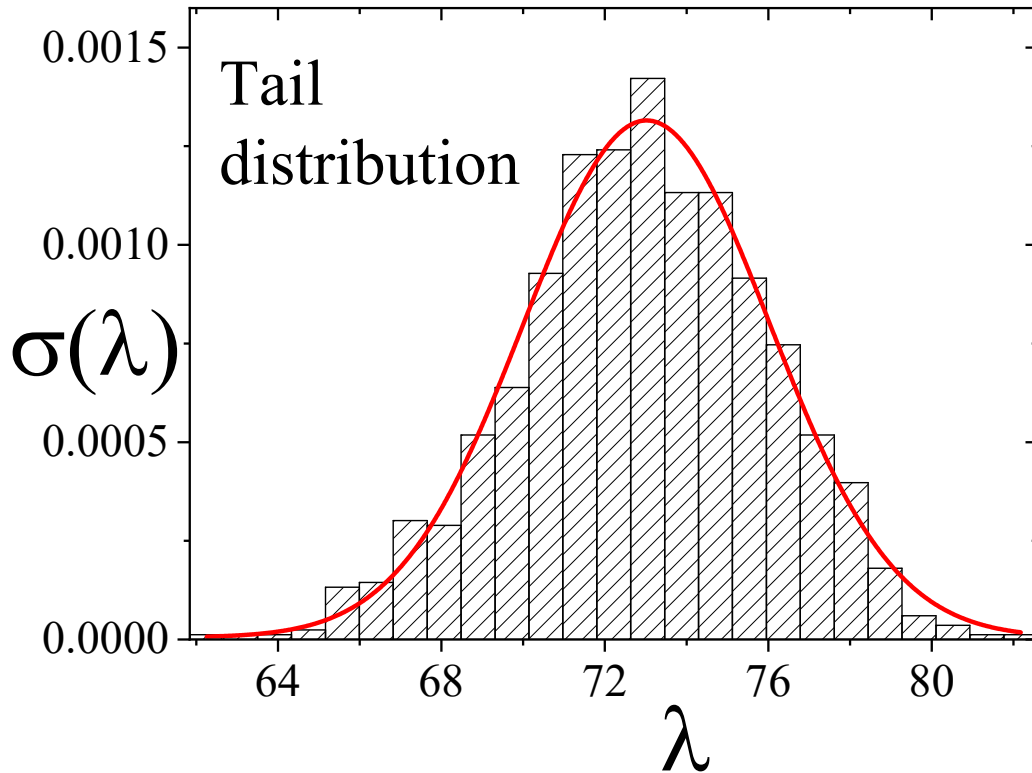


Figure 5. The Gaussian behavior stems from the eigenvalues that deviate from the bulk in Figure 4. **The eigenvalues are associated with scenarios characterized by a favorable alignment of the spins.**

from the bulk to create this Gaussian distribution – an outlier that indeed signifies a favorable alignment of the spins.

It is interesting to investigate how the density of eigenvalues behaves for  $Q = 5$  (weak first-order) and  $Q = 10$  (strong first-order). Our simulations in this case lead to results that can be observed in Figure 6.

We can observe that the gap between eigenvalues vanishes even at  $T = T_C$  for  $Q = 10$ , which does not occur for  $Q = 5$ . In the case of  $Q = 5$ , it represents a weak first-order point and mirrors the critical behavior, much like when  $Q = 5$ .

However, how this phenomenon manifests in the fluctuations of the eigenvalues is an intriguing question. When conducting simulations for  $Q \geq 5$ , a range associated with first-order transition points, The observed pattern bears a striking resemblance to the outcomes when  $Q \leq 4$ . Of course, there will be some deviations, which slightly diminish our initial surprise.

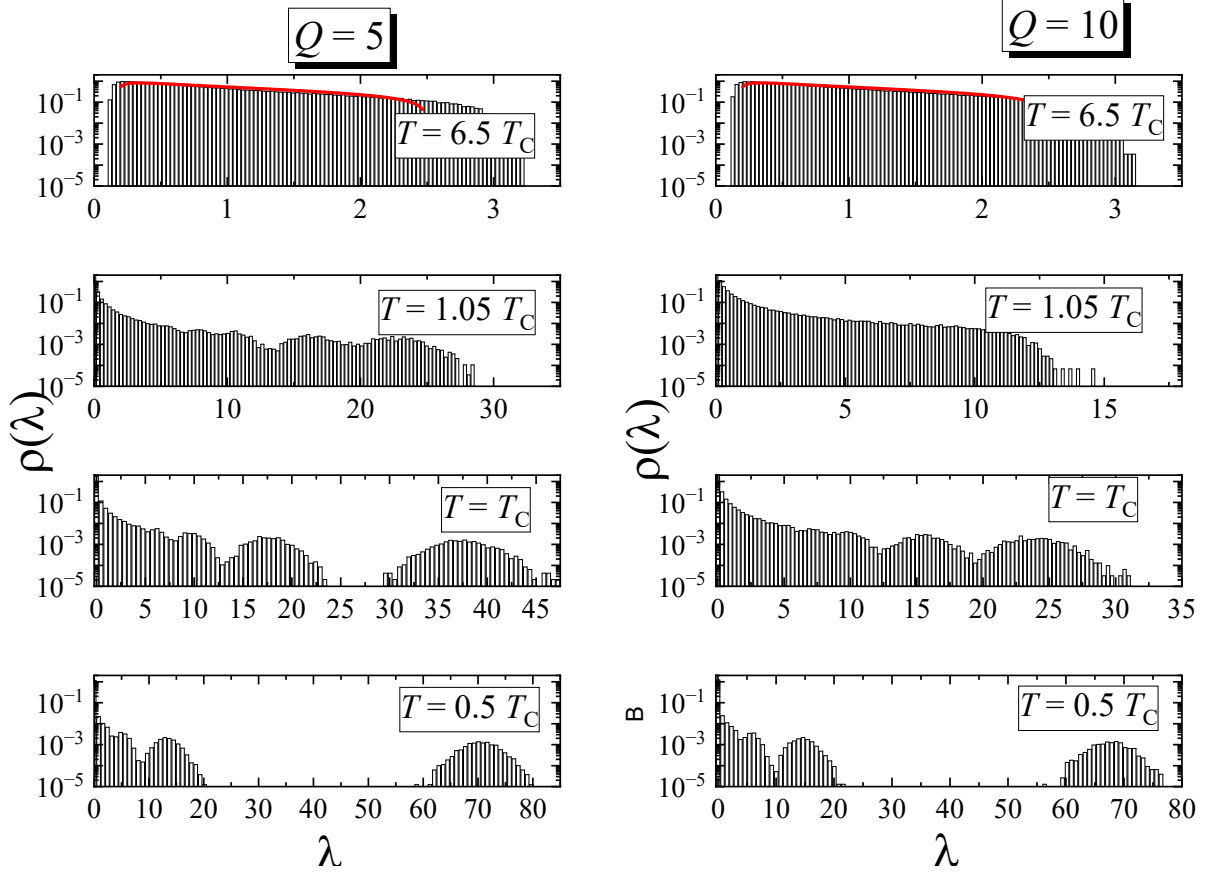


Figure 6. Density of eigenvalues for the 5-state and 10-state Potts models. The gap between eigenvalues disappears even at  $T = T_C$  for  $Q = 10$ , which does not occur for  $Q = 5$ . It is evident that  $Q = 5$  exhibits characteristics of a weak first-order point, closely reflecting the critical behavior observed when  $Q < 5$ .

To better understand the mechanism responsible for this characteristic gap closure, we aim to demonstrate that the phase transitions of the simulated magnetic system are intricately mirrored by the fluctuations of eigenvalues. It is evident that these fluctuations are influenced by the presence of these gaps.

In order to show that, we calculated the first ( $k = 1$ ) and second ( $k = 2$ ) moments. The  $k$ -th moment is given by

$$\langle \lambda^k \rangle = \frac{\sum_{i=1}^{N_{bins}} \lambda_i^k \sigma(\lambda_i)}{\sum_{i=1}^{N_{bins}} \sigma(\lambda_i)}. \quad (18)$$

Fig. 7 shows the first moment  $\langle \lambda \rangle$  as function of  $T/T_C$ . The dispersion defined as  $\langle (\Delta\lambda)^2 \rangle = \langle (\lambda - \langle \lambda \rangle)^2 \rangle$  as function of  $T/T_C$  for  $Q = 3, 4, 5, 7$ , and  $10$ , is shown in Fig. 8.

Here the result is really interesting since the average shows a minimum value in the proximity of critical temperature ( $T/T_C = 1$ ) for all studied values of  $Q$  as shown in (Fig. 7) except by  $Q \geq 7$

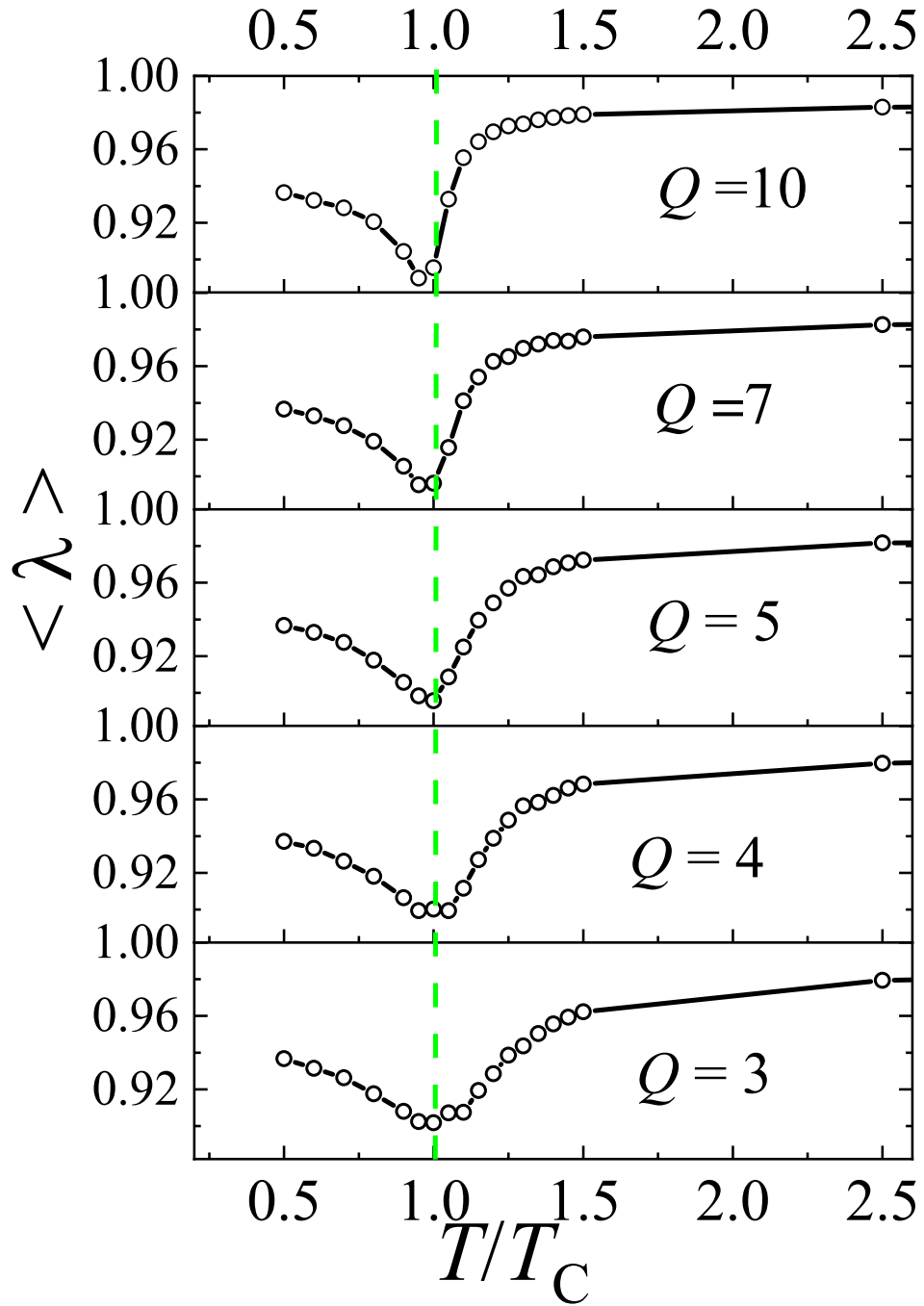


Figure 7. Averaged eigenvalue as function of  $T/T_C$  for  $Q = 3, 4, 5, 7$ , and  $10$ .

that are stronger first-order points. On the other hand, these first-order transition points (even for  $Q \geq 7$ ) are in good agreement with the inflexion points at the same phase transitions that are observed in the eigenvalue dispersion shown in (Fig 8). We have intention that assert that method

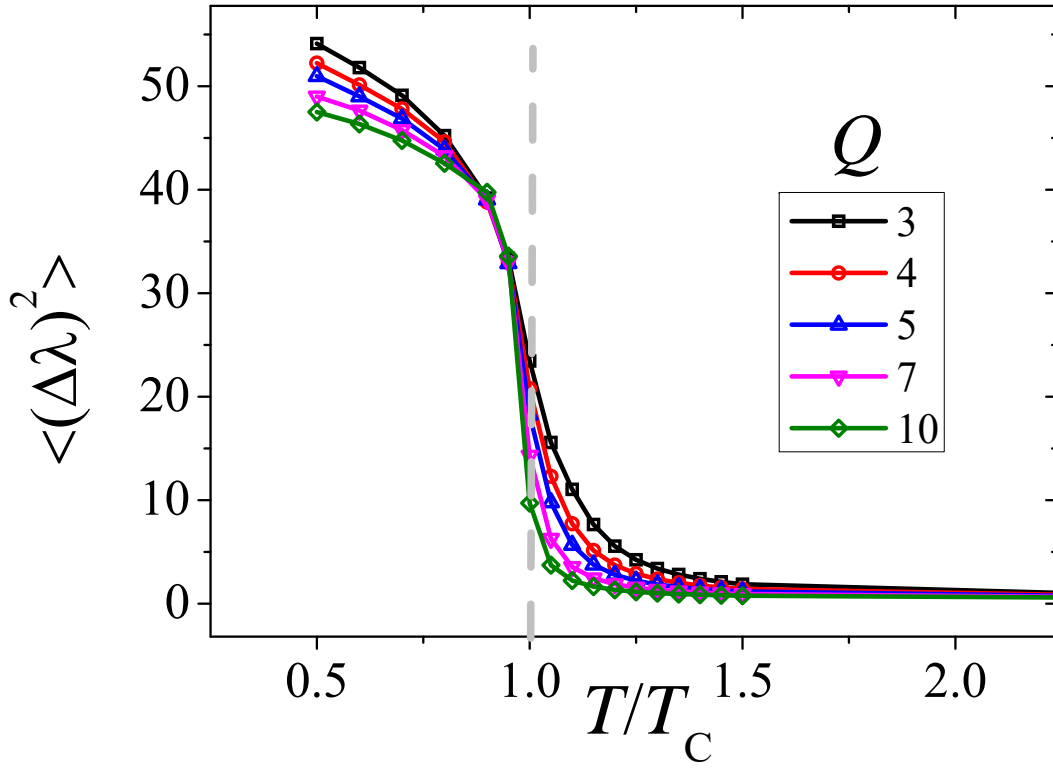


Figure 8. Dispersion of the eigenvalue as function of  $T/T_C$  for  $Q = 3, 4, 5, 7,$  and  $10$ .

can be applied to other strong first order transition and it deserves a better future exploration.

These results suggest that the eigenvalue spectra respond to the thermodynamic properties of the correspondent magnetic system. To scrutinize our results, it is interesting to check the first and second derivatives of this dispersion. Just for convenience, we have taken the derivative of the negative of dispersion. The main plot shown in Fig. 9 corresponds to the result of the derivative with the previous interpolation by splines. The inset plot is without performing the splines.

We observe a maximum at  $T = T_C$ , at most a draw for  $Q = 10$  when we do not use interpolation by splines. It is important to remember that we have a strong first-order transition point in that case.

In order to show that the method is definitively a good identifier of transition points, independent of the transition order, we compute  $T_C^2 \frac{\partial^2}{\partial T^2} \langle(\Delta\lambda)^2\rangle$ . We can observe the discontinuity of this quantity occurring exactly at transition point temperatures, as can be observed in Fig. 10.

Up to this point, we gave numerical evidence that the thermodynamics of the  $Q$ -state Potts

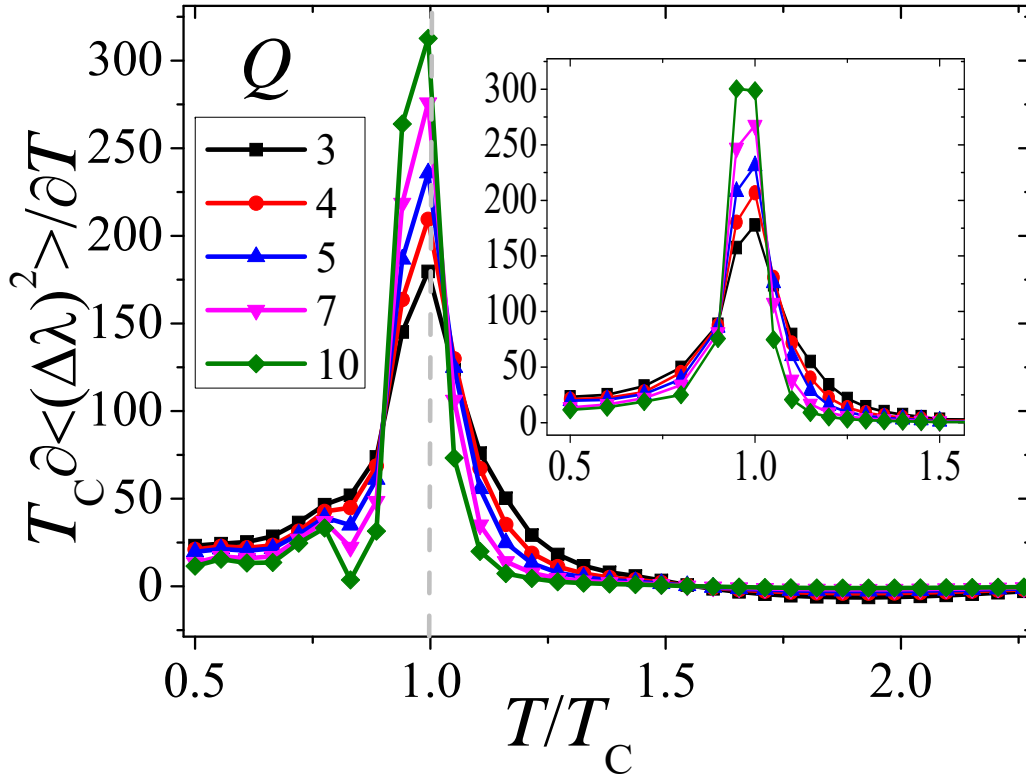


Figure 9. Derivative of negative of the dispersion as function of  $T/T_C$  for  $Q = 3, 4, 5, 7,$  and  $10$ . The main plot is the result using splines before performing the derivative. The inset plot corresponds to the same plot not using the splines.

model is dictated by the fluctuations of the eigenvalues uniquely imposed by the correlation held in the Wishart matrices. Given the role played by these correlations in the thermodynamics of the system, we need to see what happens to the correlation distribution as  $Q$  increases for different critical temperatures.

#### A. Checking of the histograms of correlation

Since we have computed the correlations  $\rho_{ij} = \frac{\langle \mathcal{M}_i \mathcal{M}_j \rangle - \langle \mathcal{M}_i \rangle \langle \mathcal{M}_j \rangle}{s_i s_j}$  between different pairs of magnetization series, where  $s_i = \sqrt{\langle \mathcal{M}_i^2 \rangle - \langle \mathcal{M}_i \rangle^2}$ , for  $i > j$ , and we perform a histogram of these elements that are identically equal  $\mathcal{G}_{ij}$  and here the interchange between symbols  $\mathcal{G}_{ij}$  by  $\rho_{ij}$  is solely for convenience. We look at situations  $T < T_C$ ,  $T = T_C$  and  $T > T_C$ , exactly in the same conditions that we used to obtain the eigenvalues of  $\mathcal{G}$ . The results are summarized and reported

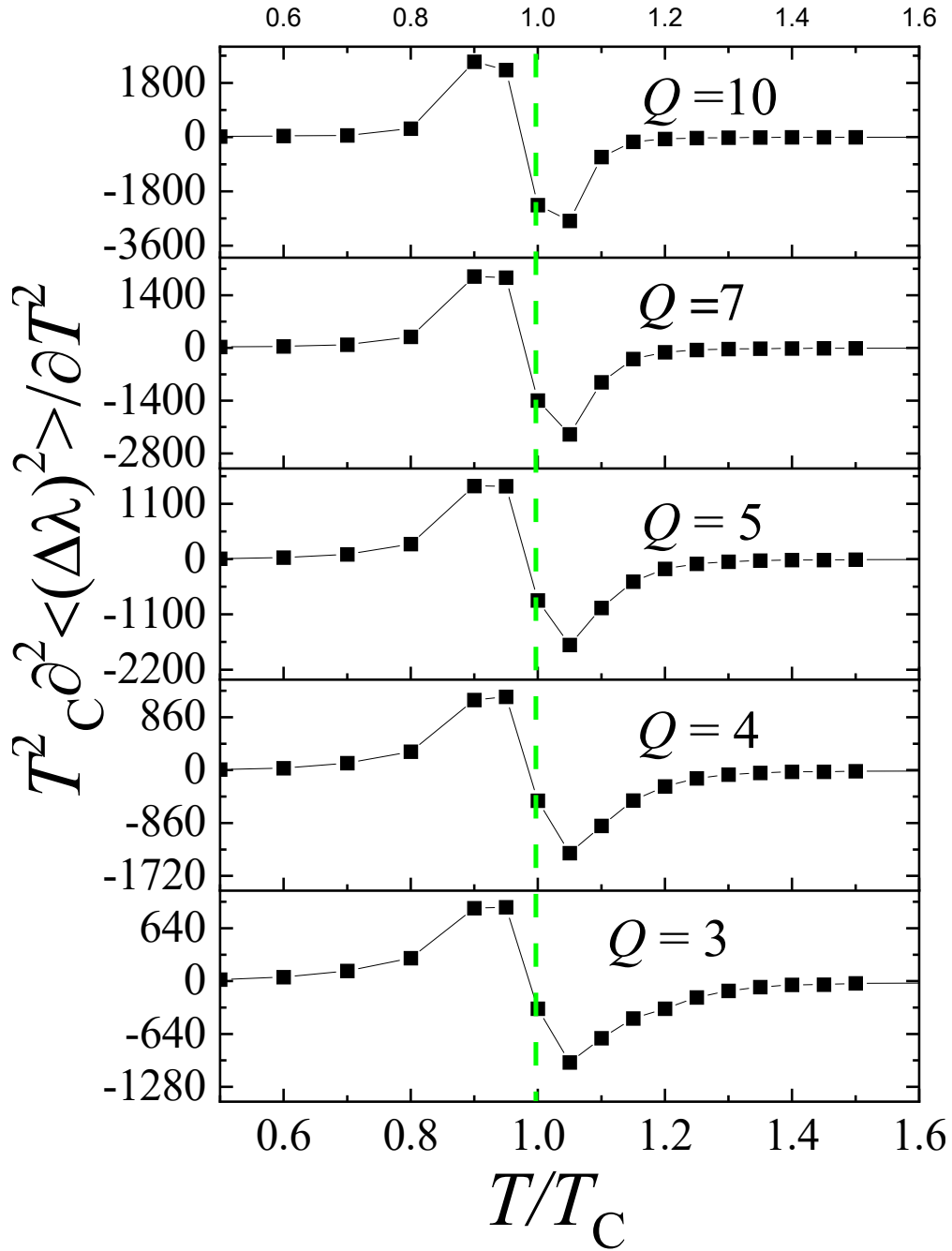


Figure 10. Second derivative of dispersion:  $T_C^2 \frac{\partial^2 \langle (\Delta\lambda)^2 \rangle}{\partial T^2}$  as function of  $T/T_C$  for  $Q = 3, 4, 5, 7,$  and  $10$ . As  $Q$  increases, the discontinuity is numerically more significant, which makes sense since the order of transition increases.

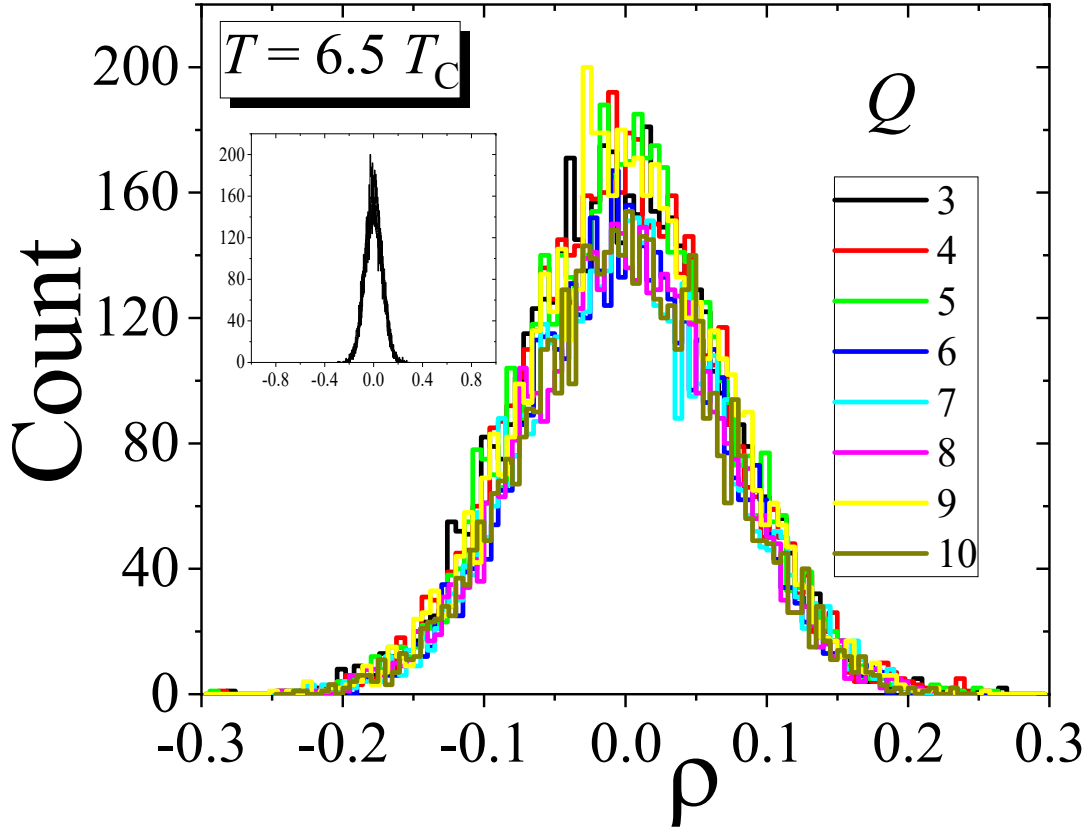


Figure 11. Histogram of correlations for  $T > T_C$ . One observes a gaussian behavior for all  $Q$  – values. The inset plot presents the same result considering a large range of correlations by showing histograms narrow indeed, around  $\rho = 0$ , which in practice means to be uncorrelated

in Figs. 11, 12, and 13.

We see that for high temperatures, as shown in Fig. 11, the system that starts with a magnetization at  $T \rightarrow \infty$ , keeps this same behavior. We can observe that for all values of  $Q$ , the gaussians are narrow exactly as expected. However, for  $T = T_C$ , Fig. 12 the system responds and acquires orientation so that the correlation follows a broad histogram with  $\rho$  in the range from  $-1$  to  $+1$  with null average. The most interesting point is the changing of this broad histogram that is almost a uniform distribution for  $Q = 3$ , going throughout a parabolic distribution (see the already first-order point  $Q = 7$ ) and finally becoming a spread gaussian for the strong first-order point ( $Q = 10$ ).

We have to emphasize the possible "indetermination" for  $Q = 4$ , perhaps indicating the existence

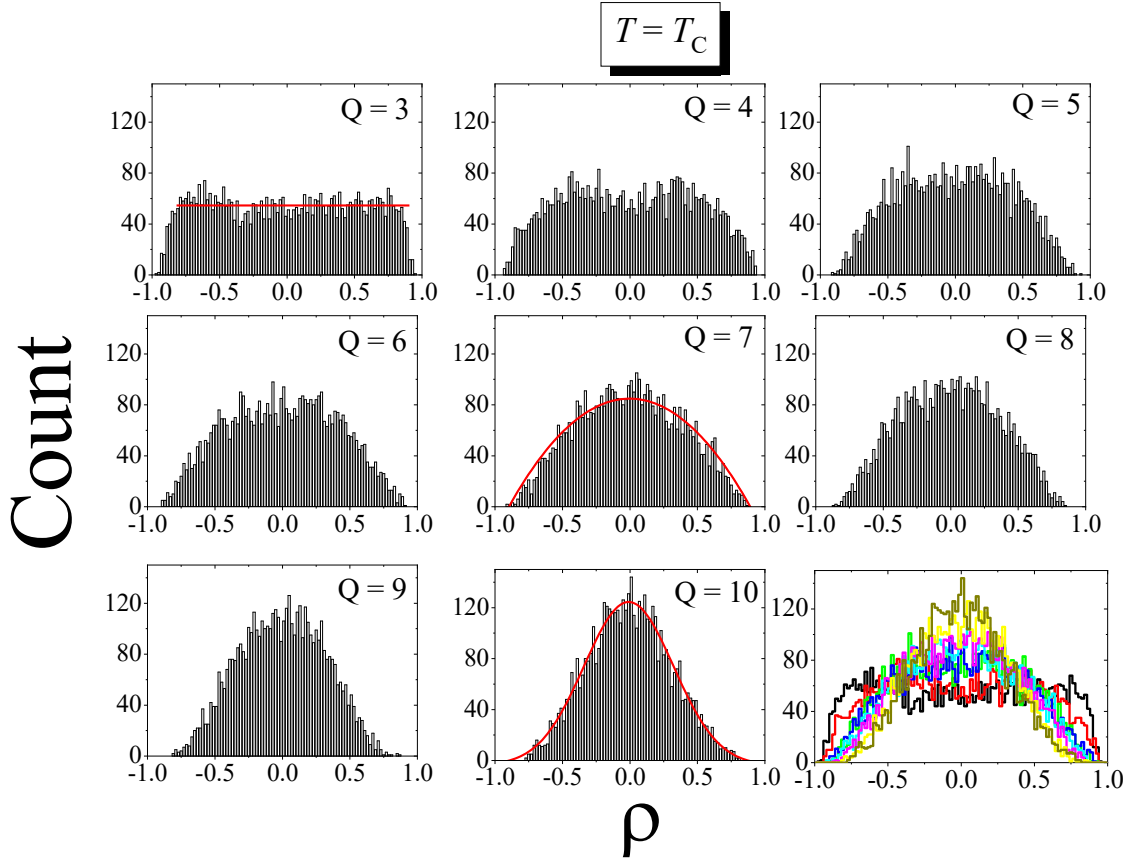


Figure 12. Histograms of the correlation for  $T = T_C$ . Here it is interesting to observe broad histograms distributed in the range  $-1 < \rho < 1$ , are observed. For  $Q = 3$  we almost have a uniform distribution of correlations. Such distribution is continuously curved until it arrives at a quadratic function ( $Q = 7$ ) which already is a first-order point. For  $Q = 10$  one has a wide gaussian. The last plot presents all previous plots jointly for comparison.

of a marginal operator for this Potts model (see [57, 60, 61]). We can finally see that for  $T < T_C$ , shown in Fig. 13, the system really acquires a strong ordering characterized by a high correlation with two pronounced peaks in  $\rho \approx -1$  and  $\rho \approx 1$ . An observation is that the peaks are higher for the second-order points. An inevitable conclusion is that the transition from a two-peaked shape to a broad gaussian-like distribution for the correlation at  $T = T_C$  between eigenvalues probably has a direct relation to a spectral interpretation of the thermodynamics of systems that present first and second-order transitions. Our approach to this kind of problem can bring new ways to deal with the thermostatics of several physical systems.



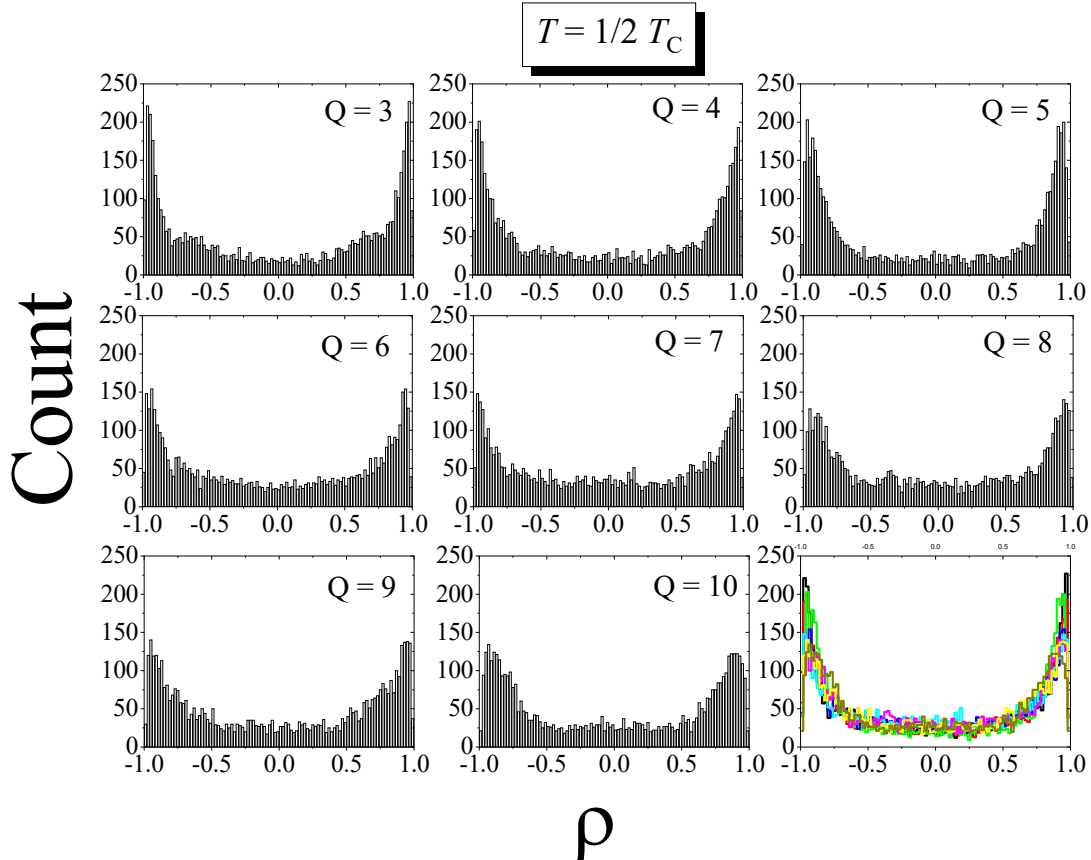


Figure 13. Histograms of the correlation for  $T < T_C$ . It is interesting to observe that independently of  $Q$ -value, one has similar behavior, double peak at  $\rho \approx 1$  and  $\rho \approx -1$ . The Last plot presents all previous histograms in the same figure or a comparison

## V. SUMMARIES AND CONCLUSIONS

We studied the spectral properties of the so-called Wishart matrices built from the time evolution of spins systems. The spectra fluctuations mimic the system's thermodynamics independent of the order of the phase transition. We used the Potts model as our test bed to assess whether the approach accurately characterizes both the second and weak first-order points. Additionally, this model allows us to investigate how the method performs in the presence of a few higher first-order points.

The phase transition occurs because the distribution of correlations changes from a two-peaked shape at low temperatures to a gaussian-like distribution for temperatures above the critical one.

From the point of view of the density of eigenvalues of Wishart matrices, we observe gaps that appear and are “healed” at proximities of transition points (continuous or discontinuous ones).

Furthermore, we conducted a preliminary investigation using random matrices artificially generated with a fixed correlation  $\rho$  between pairs of columns in the matrix. The findings suggest that the density of eigenvalues undergoes a transition: from a scenario with a pronounced gap between the eigenvalues ( $\rho \approx 0.9$ ), which diminishes as  $\rho$  decreases, until it reaches a state characterized by a unified bulk of eigenvalues at  $\rho \approx 0$ . These nuances, albeit somewhat pedagogically, provide insight into what the fluctuations of the eigenvalues might reveal in the Potts model. This is due to a direct relationship between temperature and correlation in magnetic systems.

Our results also demonstrate that the fluctuation spectra of these matrices are analogous to the direct response of the thermodynamic system, providing insights into the system's criticality and weak first-order points. Further investigations into first-order points, including other models such as the Blume-Capel or Metamagnetic model, will be a focus of our future work, since the deviations occur for the higher first order points when we analyzed  $\langle \lambda \rangle \times T/T_C$ . Additionally, the application of this method to long-range spin systems (not only that ones in mean-field [49]) holds promise and warrants exploration in future studies.

It is crucial to emphasize that the conclusions drawn in this paper are highly reliable and not influenced by finite size scaling (FSS) issues or similar factors. For instance, readers should note that in Figure 6, the gap vanishes for  $Q = 10$  but not for  $Q = 5$ , potentially due to FSS effects. However, as depicted in Figure 14, this assumption does not hold true.

In this figure, it's evident that there is negligible difference in the density of states between  $L = 100$  and  $L = 120$ . To dispel any doubts regarding the adequacy of our chosen lattice size for the method, the inset plot within the same figure depicts the eigenvalue variance across these identical lattice sizes. Similarly, no discernible visual distinctions are observed between these two lattice sizes.

Last, but not least, we emphasize that the method presented in this paper works with lower computational complexity compared to other similar methods. It diagonalizes matrices of size  $O(N_{sample})$ , where  $N_{sample}$  is 100, for example, in this contribution. This is in contrast to other methods that require diagonalizing matrices of size  $O(L^d)$ , where  $L$  is the linear dimension of the system and  $d$  is its dimensionality. For a system with  $L = 100$  and  $d = 2$ , this would mean diagonalizing matrices of size  $10^4 \times 10^4$ .

- 
- [1] H. B. Callen, Thermodynamics and an Introduction to Thermostatistics, Wiley (1985)
  - [2] M. J. de Oliveira, Equilibrium thermodynamics, Springer (2017)

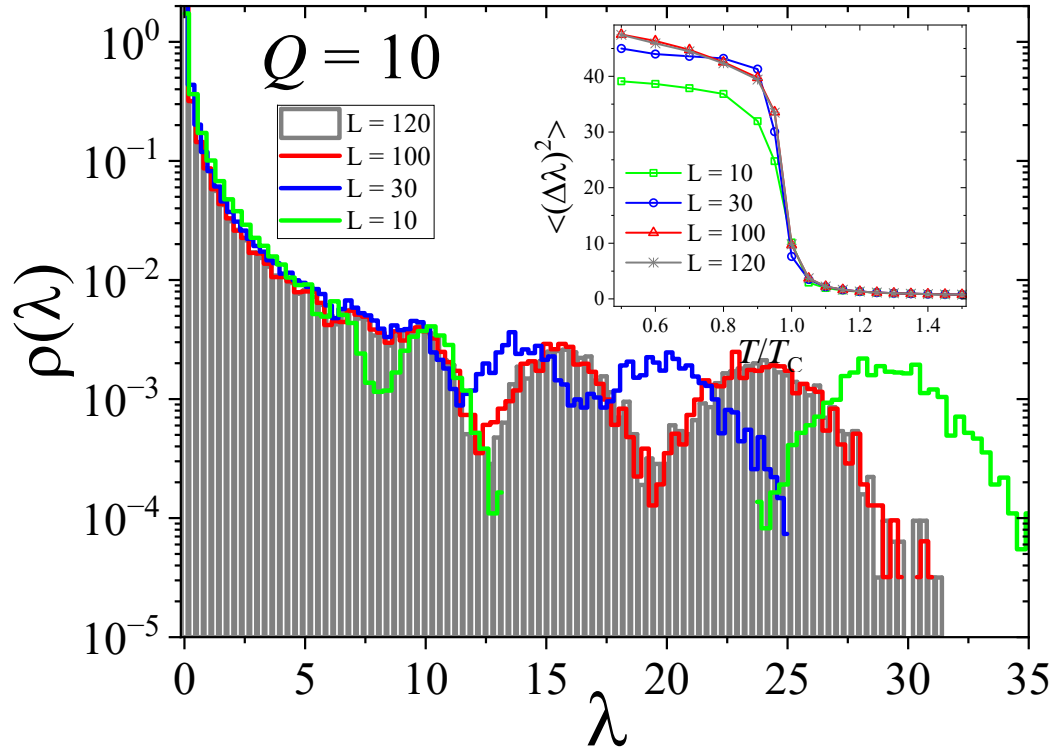


Figure 14. Finite size scaling effects on the density of eigenvalues for  $Q = 10$ . Notably, there is negligible variation between  $L = 100$  and  $L = 120$ . The inset plot illustrates the variance across these distinct lattice sizes. Likewise, comparable observations are noted for the two largest lattices.

- [3] S. R. A. Salinas Introduction to Statistical Physics, Springer (2001)
- [4] E. P. Wigner, Characteristic Vectors of Bordered Matrices with Infinite Dimensions I, Ann. Math. **62**, 548–564 (1955)
- [5] E. P. Wigner, Characteristic Vectors of Bordered Matrices with Infinite Dimensions II, Ann. Math. **65**, 203–207 (1957)
- [6] E. P. Wigner, On the Distribution of the Roots of Certain Symmetric Matrices, Ann. Math. **67**, 325–327 (1958)
- [7] M. L. Mehta, Random Matrices, Academic Press, Boston (1991)
- [8] F.J. Dyson, Statistical Theory of the Energy Levels of Complex Systems I, J. Math. Phys. **3**, 140–156 (1962)
- [9] F.J. Dyson, Statistical Theory of the Energy Levels of Complex Systems II, J. Math. Phys. **3**, 157–165 (1962)
- [10] F.J. Dyson, Statistical Theory of the Energy Levels of Complex Systems III, J. Math. Phys. **3**, 166–175

(1962)

- [11] J. Wishart, The Generalised Product Moment Distribution in Samples from a Normal Multivariate Population, *Biometrika* **20A**, 32–52 (1928)
- [12] Vinayak, T. H. Seligman, Time series, correlation matrices and random matrix models, *AIP Conf. Proc.* **1575**, 196–217 (2014)
- [13] G. Livan, M. Novaes, P. Vivo, *Introduction to Random Matrices, Theory and Practice*, Springer (2018)
- [14] S. S. Wilks, *Mathematical Statistics*, Wiley, New York (1962)
- [15] R. J. Muirhead, *Aspects of Multivariate Statistical Theory*, Wiley Series in Probability and Statistics (2009)
- [16] T. Guhr, A. Muller-Groeling, H. A. Weidenmuller, Random-matrix theories in quantum physics: common concepts, *Phys. Rep.* **299**, 189–425 (1998)
- [17] V. A. Marcenko, L. A. Pastur, Distribution of Eigenvalues for Some Sets of Random Matrices, *Math. USSR Sb.* **1** 457 (1967)
- [18] C. Recher, M. Kieburg, T. Guhr, Eigenvalue Densities of Real and Complex Wishart Correlation Matrices, *Phys. Rev. Lett.* **105**, 244101 (2010)
- [19] T. Wirtz, T. Guhr, Distribution of the Smallest Eigenvalue in the Correlated Wishart Model, *Phys. Rev. Lett.* **111**, 094101 (2013)
- [20] T. Wirtz, M. Kieburg, T. Guhr, Asymptotic coincidence of the statistics for degenerate and non-degenerate correlated real Wishart ensembles, *J. Phys. A* **50**, 235203 (2017)
- [21] F. Gotze, A.N. Tikhomirov, Rate of Convergence of the Expected Spectral Distribution Function to the Marchenko – Pastur Law, [arXiv:1412.6284](https://arxiv.org/abs/1412.6284) (2014)
- [22] I. K. Kostov,  $O(n)$  Vector Model on a Planar Random Lattice: Spectrum of Anomalous Dimensions, *Mod. Phys. Lett. A* **4**, 217 (1989)
- [23] G. M. Cicuta, L. Molinari, E. Montaldi, Multicritical points in matrix models, *J. Phys. A* **23**, L421 (1990)
- [24] J. Baik, G. B. Arous, S. Pechet, Phase transition of the largest eigenvalue for nonnull complex sample covariance matrices, *Ann. Probab.* **33**, 1643 (2005)
- [25] F. Benaych-Georges, A. Guionnet, M. Maida, Fluctuations of the Extreme Eigenvalues of Finite Rank Deformations of Random Matrices, *Electron. J. Probab.*, **16** 1621 (2011)
- [26] V. Plerou, P. Gopikrishnan, B. Rosenow, L. N. Amaral, H. E. Stanley, Universal and Nonuniversal Properties of Cross Correlations in Financial Time Series, *Phys. Rev. Lett.* **83**, 1471–1474 (1999)
- [27] V. Plerou, P. Gopikrishnan, B. Rosenow, L. N. Amaral, H. E. Stanley, A random matrix theory approach to financial cross-correlations, *Physica A* **287**, 374–382 (2000)
- [28] H.E. Stanley, P. Gopikrishnan, V. Plerou, L.A.N. Amaral, Quantifying fluctuations in economic systems by adapting methods of statistical physics, *Physica A* **287** 339–361 (2000)
- [29] L. Laloux, P. Cizeau, M. Potters, J-P. Bouchaud, Random matrix theory and financial correlations, *Int. J. Theor. Appl. Finance* **3**, 391 (2000)

- [30] J-P. Bouchaud, M. Potters, Theory of Financial Risks. From Statistical Physics to Risk Management, University Press, Cambridge (2000)
- [31] A.M. Sengupta, P.P. Mitra, Distributions of singular values for some random matrices, Phys. Rev. E **60** 3389 (1999)
- [32] I. Johnstone, D. Paul, PCA in high dimensions: An orientation, Proc. IEEE, **106**, 1277 (2018)
- [33] T. Vinayak, T. Prosen, B. Buca, T. H. Seligman, Spectral analysis of finite-time correlation matrices near equilibrium phase transitions, EPL **108**, 20006 (2014)
- [34] S. Biswas, F. Leyvraz, P.M. Castellero, T.H. Seligman, Rich structure in the correlation matrix spectra in non-equilibrium steady states, Nat. Sci. Rep. **7** 40506 (2017)
- [35] B. Zheng, Monte Carlo simulations of short-time critical dynamics, Int. J. Mod. Phys. B **12**, 1419 (1998)
- [36] D. A. Huse, Remanent magnetization decay at the spin-glass critical point: A new dynamic critical exponent for nonequilibrium autocorrelations, Phys. Rev. B **40**, 304 (1989)
- [37] H. K. Janssen, B. Schaub, B. Schmittmann, New universal short-time scaling behaviour of critical relaxation processes, Z. Phys. B: Condens. Matter **73**, 539 (1989)
- [38] H. K. Janssen, K. Oerding, Non-equilibrium relaxation at a tricritical point, J. Phys. A: Math. Gen. **27**, 715 (1994)
- [39] T. Tome, M. J. de Oliveira, Short-time dynamics of critical nonequilibrium spin models, Phys. Rev. E **58**, 4242 (1998)
- [40] T. Tome, J. R. Drugowich de Felicio, Short Time Dynamics of an Irreversible Probabilistic Cellular Automaton, Mod. Phys. Lett. B, **12**, 873 (1998)
- [41] M. Santos, W. Figueiredo, Short-time dynamics of a metamagnetic model, Phys. Rev. E **62**, 1799 (2000)
- [42] E. V. Albano, M. A. Bab, G. Baglietto, R. A. Borzi, T. S. Grigera, E. S. Loscar, D. E. Rodriguez, M. L. R. Puzzo, G. P. Saracco, Study of phase transitions from short-time non-equilibrium behaviour, Rep. Prog. Phys. **74**, 026501 (2011)
- [43] M. Henkel, M. Pleimling, Non-equilibrium Phase Transitions, Vol. 2: Ageing and Dynamical Scaling far from Equilibrium, Springer, Dordrecht (2010)
- [44] L. C. de Souza, A. J. F. de Souza, M. L. Lyra, Hamiltonian short-time critical dynamics of the three-dimensional XY model, Phys. Rev. E **99**, 052104 (2019)
- [45] S. Z. Lin and B. Zheng, Short-time critical dynamics at perfect and imperfect surfaces, Phys. Rev. E **78**, 011127 (2008)
- [46] R. da Silva, Exploring the Similarities Between Mean-field and Short-range Relaxation Dynamics of Spin Models, Braz. J. Phys. **52**, 128 (2022)
- [47] R. da Silva, M. J. de Oliveira, T. Tome, and J. R. Drugowich de Felicio, Analysis of earlier times and flux of entropy on the majority voter model with diffusion, Phys. Rev. E **101**, 012130 (2020)
- [48] R. da Silva, Random matrices theory elucidates the nonequilibrium critical phenomena, Int. J. Mod.

- Phys. C, **2350061** 1 (2023)
- [49] R. da Silva, H. C. M. Fernandes, E. Venites Filho, S. D. Prado, J. R. Drugowich de Felicio, Mean-field criticality explained by random matrices theory, *Braz. J. Phys.* **53**, 80 (2023)
- [50] R. da Silva, S. D. Prado, A simple study of the correlation effects in the superposition of waves of electric fields: The emergence of extreme events, *Phys. Lett. A* **384**, 126231 (2020)
- [51] R. da Silva, E. Venites Filho, A. Alves, A thorough study of the performance of simulated annealing in the traveling salesman problem under correlated and long tailed spatial scenarios, *Physica A* **577**, 126067 (2021)
- [52] A. Bloemendal, B. Virag, Limits of spiked random matrices I, *Probab. Theory Relat. Fields.* **156**, 795-825 (2013)
- [53] A. Bloemendal, B. Virag, Limits of spiked random matrices II, *Ann. Probab.* **44**, 2726 (2016)
- [54] M. Y. Mo, The rank 1 real Wishart spiked model I. Finite N analysis, arXiv:1011.5404 (2010)
- [55] M. Y. Mo, The rank 1 real Wishart spiked model, arXiv:1101.5144 (2011)
- [56] F. Y. Wu, The potts model, *Rev. Mod. Phys.* **54**, 235 (1982)
- [57] R. da Silva, J. R. Drugowich de Felicio, Critical dynamics of the Potts model: short-time Monte Carlo simulations, *Phys. Lett. A* **333**, 277 (2004)
- [58] G. Forgacs, S. T. Chui, H. L. Frisch, Critical dynamics of the Potts model, *Phys. Rev. B* **22**, 415 (1980)
- [59] T. Martyneć, S. H. L. Klapp, S. A. M. Loos, Entropy production at criticality in a nonequilibrium Potts model, *New J. Phys.* **22** 093069 (2020)
- [60] R. H. Swendsen, D. Andelman, A. N. Berker, Critical exponents and marginality of the four-state Potts model: Monte Carlo renormalization group, *Phys. Rev. B* **24**, 6732 (1981)
- [61] L. P. Kadanoff, F. J. Wegner, Some critical properties of the eight-vertex model, *Phys. Rev. B* **4**, 3989 (1971)